

# Synthesis and characterization of hydroxyapatite by microwave heating using $\text{CaSO}_4 \cdot 2\text{H}_2\text{O}$ and $\text{Ca}(\text{OH})_2$ as calcium source

Ion Teoreanu · Maria Preda · Alina Melinescu

Received: 18 April 2006 / Accepted: 1 November 2006 / Published online: 10 July 2007  
© Springer Science+Business Media, LLC 2007

**Abstract** In this paper, synthesis of hydroxyapatite (HAp) in the absence or presence of 1.05 wt% magnesium oxide, as sintering additive, by heating in a microwave oven was studied. For this purpose,  $\text{CaSO}_4 \cdot 2\text{H}_2\text{O}$ ,  $\text{Ca}(\text{OH})_2$ ,  $\text{Mg}(\text{OH})_2$  and  $(\text{NH}_4)_2\text{HPO}_4$  were used as raw materials. The total chemical reactions for all the studied compositions were observed after a 3 h microwave treatment. In case of pure hydroxyapatite, a powder with needle-like grains results. In the presence of  $\text{Mg}(\text{OH})_2$ , the  $(\text{Mg}, \text{Ca}_2) \cdot \text{O} \cdot (\text{HPO}_4)_2 \cdot \text{H}_2\text{O}$  hydrated phosphate is formed besides hydroxyapatite. Pure hydroxyapatite, thermally treated at 1,200 °C, mostly transforms in  $\beta\text{-Ca}_3\text{P}_2\text{O}_8$ . By adding MgO into the precursor mixture, hydroxyapatite was stabilised, and found in a much greater proportion at 1,200 °C. After the thermal treatment, the hydroxyapatite, analysed by electronic microscopy, shows a prismatic morphology originating in its initial state.

## Introduction

The ability of dielectric materials to absorb microwaves (MW) and to transform electromagnetic energy into heat represents a good alternative technology to the conventional heating. This way of conversion technique is based on intrinsic properties of dielectric materials like dielectric

permittivity and tangent of the loss angle. The ratio between these properties defines the ability of the material to transform, at a given frequency, the electromagnetic energy into heat [1]. The main advantages of the method consist in the great heating rate, a homogenous temperature in the entire reaction volume and in the absence of the direct contact between the energy source and the reaction mixture.

Different microwave routes were previously described in the literature. The general aim of these works was to obtain a Ca/P ratio close to 1.667, the theoretical value. Parhi and co-workers [2] synthesized hydroxyapatite using a stoichiometric ratio of  $\text{CaCl}_2$  and  $\text{Na}_3\text{PO}_4$ . The initial mixture was heated 30 min in the microwave oven. The final product was subsequently washed to eliminate the chloride also formed in the reaction. The HAp formation was proved by X-ray diffraction and further, scanning electronic microscopy (SEM) revealed the formation of spherical grains of about 100 nm diameter. Komarneni and Katsuki [3] showed a rapid kinetics of the HAp synthesis from an initial mixture of  $\text{CaSO}_4 \cdot 2\text{H}_2\text{O}$  and  $(\text{NH}_4)_2\text{HPO}_4$  at 195 °C. In this case, SEM revealed needle-like crystals of HAp with lengths of less than 200 nm. D.S.R. Krisna et al. [4] prepared HAp, by hydrolysis of  $\beta\text{-Ca}_3\text{P}_2\text{O}_8$  as a water suspension. They added fluorhydric acid to the initial mixture and micro waved it for 5–40 min. This resulted in a fluorinated HAp, lacking in calcium. Other groups started from  $\alpha\text{-Ca}_3\text{P}_2\text{O}_8$  and used microwaves to heat the initial reaction mixture to 70–80 °C. They obtained hydroxyapatite crystals with lengths of 30–300 nm and width of 5–50 nm [5], thus being in good agreement with other studies [6–7] that reported HAp formation by microwave heating in water suspensions. One should pay close attention to the HAp characterization since slight changes in the reaction conditions can greatly influence the Ca/P ratio and subse-

I. Teoreanu · M. Preda · A. Melinescu (✉)  
Science and Engineering of Oxide Materials and Nanomaterials,  
Politehnica University of Bucharest, 1-7, Gheorghe Polizu Str.,  
Bucharest 011061, Romania  
e-mail: alina.melinescu@gmail.com

quently lead to different behaviour during thermal treatment. FTIR [8–16] is one of the most sensitive methods used to prove the presence or absence of other phosphates beside HAp. This method can detect traces of such impurities as well as the existence of additional ionic groups to HAp such as carbonate ion.

There is a very good correlation between HAp stability and Ca/P ratio and it was found that HAp is stable only when Ca/P ratio has the theoretical value [16]. Thermal treatment studies of HAp showed water loss and pore formation temperatures greater than 800–900 °C. In order to improve sintering ability of HAp different work conditions and trace additives (such as Na<sub>2</sub>O, Li<sub>2</sub>O, MgO etc.) were used.

Gibson et al. [17] studied the effect of the pressure on HAp sintering and they established that this begins at 800–900 °C or at 1000–1050 °C for low or well-crystallised HAp. Measured temperature for 96% from theoretical density was with 150–200 °C lower for hydroxyapatite with a low crystalline degree in comparison with a HAp good crystallized. Fanovici and Porto Lopez [18] used lithium and magnesium oxide as sintering additives. They found that Li<sub>2</sub>O leads to the apparition of a liquid phase in the sintering process, which represents a lithium–calcium–phosphate glass. A small lithium oxide proportion the increase of the relative density determined, but at a higher content this is dramatically reduced with the formation of great size pores. If MgO was used as additive, important changes were not noticed on the sintering degree, but it was shown that this oxide partially was solubilized in Ca<sub>3</sub>P<sub>2</sub>O<sub>8</sub> lattice and a decreasing of the size grain was observed. Another sintering additive was Na<sub>2</sub>O [19] and was reported that this oxide could penetrate into HAp lattice and it's stabilised. At the same time with Na<sup>+</sup> penetration into the lattice, a partial substitution of PO<sub>4</sub><sup>3-</sup> with CO<sub>3</sub><sup>2-</sup> ion was noticed to compensate the electric charge. In the papers [20, 21] starting from commercial-grade HAp as raw material, studied MgO as sintering additive, in correlation with thermal equilibrium diagram.

Although, many papers reported on the HAp synthesis the results are not in good agreement and do not totally explain HAp stability as a function of temperature. In this research HAp with or without MgO as additive was synthesised by microwave heating and the behaviour of powders at thermal treatment was investigated.

## Experimental

Stoichiometric and partially substituted magnesium HAp, with 1.05% wt% MgO, were prepared from CaSO<sub>4</sub>·2H<sub>2</sub>O, Ca(OH)<sub>2</sub>, Mg(OH)<sub>2</sub> and a 0.5 M (NH<sub>4</sub>)<sub>2</sub>HPO<sub>4</sub> solution. Calcium sulphate and the hydroxides were used in solid state. The ammonium phosphate solution was dropwise added into the reaction mixture and the suspension was stirred vigorously. The initial pH was raised to 10 by using 25% ammonium hydroxide (solution). A microwave oven with 2.45 GHz frequency and 150 W power was used. The samples were thermally treated for 1–3 h. The resulted precipitates were subsequently at 300 °C in order to remove the water and the ammonium sulphate formed in the reaction. The pellets were uniaxially pressed at 1000 daN/cm<sup>2</sup>, and then thermally treated in an electrical furnace, at 1,200 °C, for maximum 1 h. The nature of crystalline phases was determined, before and after thermal treatment by X-ray patterns diffraction in reflexion mode, with CuK<sub>α</sub> radiation (Shimadzu XRD Diffractometer). The FT-IR spectra were taken between 460 cm<sup>-1</sup> and 4,600 cm<sup>-1</sup> in KBr (spectral resolution of 4 cm<sup>-1</sup>) on a Shimadzu FTIR 8400 Spectrophotometer. Scanning electron microscopy (Hitachi S 2600 N) was used to investigate the morphology and particle size of the synthesized powders.

## Results and discussions

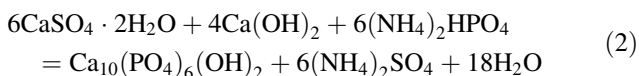
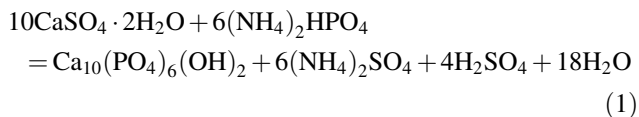
### The synthesis of powders

The composition of synthesized powders is presented in Table 1, where the first column presents HAp with stoichiometric composition. The second column presents a mixture constituted to 95% HAp and 5% of a ternary Ca<sub>3</sub>Mg<sub>3</sub>P<sub>4</sub>O<sub>16</sub> compound with 1.05 wt% MgO content. The ternary compound was chosen according to the phase diagram of the Ca<sub>3</sub>Mg<sub>3</sub>P<sub>4</sub>O<sub>16</sub>-HAp pseudosystem and because it fuses below 1200 °C (thermal treatment temperature) thus being compatible with HAp. We used commercial-grade HAp as starting material since it was demonstrated that the sintering degree remains practically unchanged above 1,200 °C [21]. Since magnesium oxide is also contained in bones, it cannot negatively influence the biological properties of HAp if used as additive.

**Table 1** The mineralogical and oxide composition of synthesised samples

Sample	Mineralogical composition, %		Oxide composition, %			
	Ca <sub>10</sub> (PO <sub>4</sub> ) <sub>6</sub> (OH) <sub>2</sub>	3CaO·3MgO·2P <sub>2</sub> O <sub>5</sub>	CaO	P <sub>2</sub> O <sub>5</sub>	H <sub>2</sub> O	MgO
1	100	–	55.77	42.44	1.79	–
2	95	5	54.46	42.79	1.70	1.05

For the synthesis following two types of reactions were used in order to synthesize our materials:



For the sample with 1.05% MgO only the reaction (2) was used.

Characterization of the reaction products

Mineralogical composition of synthesized powders

X-ray diffraction was used to investigate the mineralogical composition of the synthesized powders. Figure 1 presents the X-ray spectrum for sample 1, prepared by reaction (1).

The spectrum presented in Fig. 1 reveals the presence of two hydrated phosphates, CaHPO<sub>4</sub> and CaHPO<sub>4</sub>·3H<sub>2</sub>O. The specific peaks of HAp (at this value) are missing because the resulted H<sub>2</sub>SO<sub>4</sub> (reaction 1) changed the initial pH (from basic to acid) thus inhibiting the formation of HAp. Reaction (2) was used in order to avoid this problem. In this case, CaSO<sub>4</sub> was partially substituted with Ca(OH)<sub>2</sub>, thus obtaining only ammonium sulphate which does not decrease the pH. Reaction (2) was carried out between 1 h and 3 h. The X-ray diffraction spectrum for the sample 1, after 1 h reaction, shows two crystalline phases: CaHPO<sub>4</sub> and Ca(OH)<sub>2</sub> (Fig. 2).

By increasing the reaction time to 2 h we obtained mostly HAp and traces of calcite, proved by X-ray

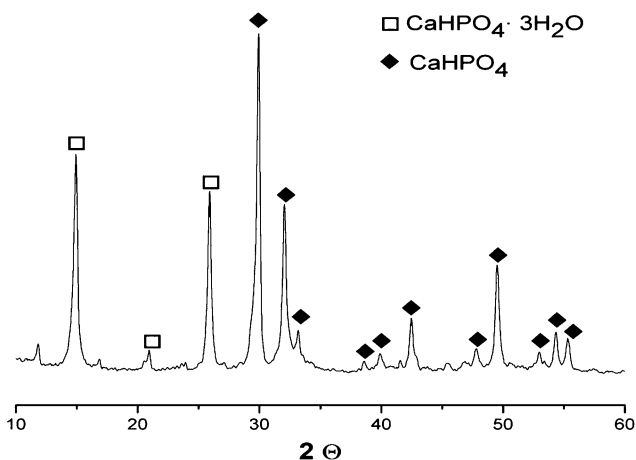


Fig. 1 XRD patterns for the sample 1, synthesised by reaction (1), with heating in microwave oven and 1 h plateau

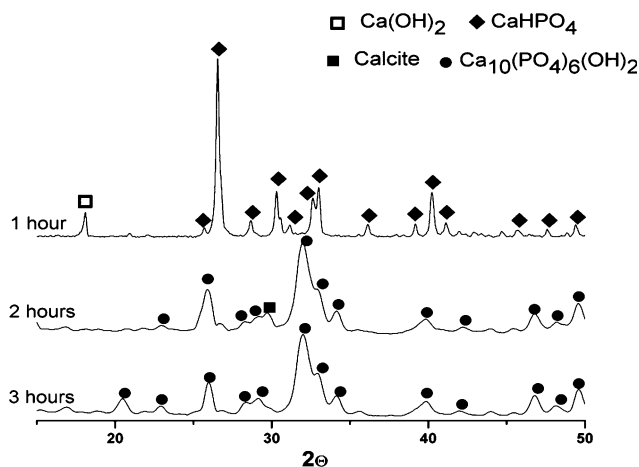


Fig. 2 XRD patterns of sample 1, synthesised by the reaction (2) versus the time of microwave heating

diffraction. After 3 h reaction time, the sample practically contains only HAp (see Fig. 2). Thus CaHPO<sub>4</sub> is just an intermediate phase, which afterwards reacts with the excess of Ca(OH)<sub>2</sub>, to form HAp. Figure 3 presents the X-ray spectrum for the sample 2. One can observe the presence of two crystalline phases, the major compound HAp and traces of (Mg, Ca)<sub>2</sub>·O·(HPO<sub>4</sub>)<sub>2</sub>·H<sub>2</sub>O.

The reaction products were also analysed by FTIR spectrometry (Fig. 4), and the results were compared with recent literature data [8–16].

The 569 and 604 cm<sup>-1</sup> bands were observed and they were assigned to [PO<sub>4</sub>]<sup>3-</sup> from hydroxyapatite. The 667 cm<sup>-1</sup> band represent a characteristic line of HO<sup>-</sup> ion from same compound. The presence of three sharp peaks in the same region demonstrates a high degree of crystallinity for HAp. We also identified IR resonances at 1,038, 1,103, 1,149 cm<sup>-1</sup> which are specific for the [PO<sub>4</sub>]<sup>3-</sup> ion. The

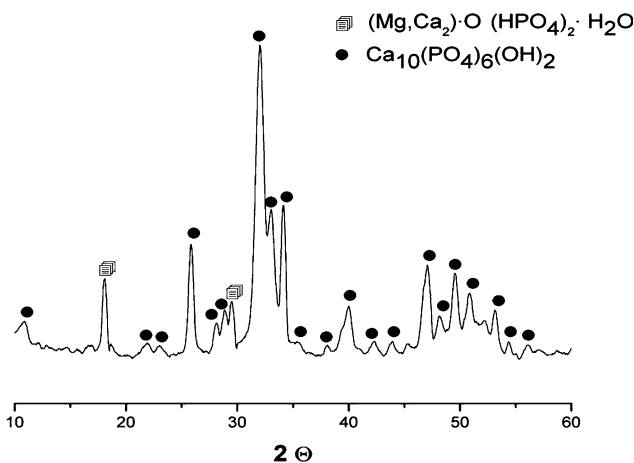
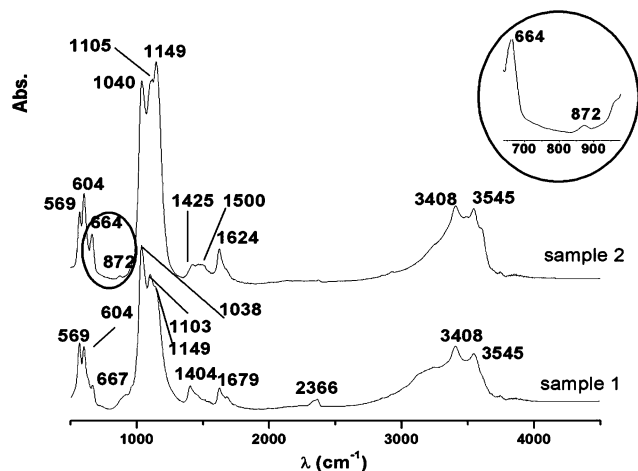


Fig. 3 XRD patterns of the sample 2, synthesised by reaction (2) and maintained a plateau of 3 h in microwave field



**Fig. 4** FTIR spectra of synthesised powders sample 1—after 3 h of heating in microwave oven; sample 2—with MgO as additive, after 3 h of heating in microwave oven

resonance centred at  $3,545\text{ cm}^{-1}$  corresponds to  $[\text{HO}]^-$  ion from HAp lattice. The large peak between  $2,500\text{ cm}^{-1}$  and  $3,700\text{ cm}^{-1}$  represents the vibration modes of the water molecule retained on the HAp surface by hydrogen bonds. The  $1,404\text{ cm}^{-1}$  band and the large resonance between  $1,425\text{ cm}^{-1}$  and  $1,500\text{ cm}^{-1}$  can be assigned to  $\text{CO}_3^{2-}$  ion, which partially substitutes the  $\text{PO}_4^{3-}$  ion in HAp lattice. When magnesium hydroxide was used in the reaction, the presence of a new peak at  $872\text{ cm}^{-1}$  was noticed. This is characteristic for the  $\text{HPO}_4^{2-}$  group from double phosphate of calcium and magnesium, also identified by X-ray diffraction.

#### The morphology of the synthesised powders

The two types of powders obtained after 3 h of thermal treatment in the microwave oven were examined by scanning electron microscopy. The micrographs for sample 1, obtained by the route 2, are shown in the Fig. 5a, b.

One can notice the presence of agglomerates with needle-like shape, with a length of about  $10\text{--}20\text{ }\mu\text{m}$ , which indicates the fact that, they must be milled before sintering, to destroy the porous microstructure. This agglomeration appears as a result of weak hydrogen bonds, due to the existence of  $\text{HO}^-$  groups in the lattice of Hap. This matches the results obtained by other authors [5, 6]. In the case of the powder that contains MgO, agglomerates of needle-like grains result but with smaller sizes (Fig. 6a, b).

#### Behaviour at sintering thermal treatment. Description of the sintered samples

The pellets from synthesised powders were thermally treated at  $1,200\text{ }^\circ\text{C}$ , temperature at which the sintering

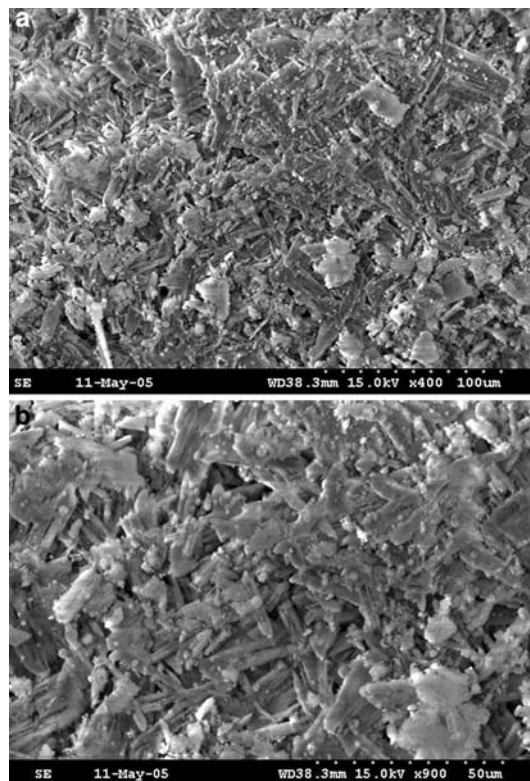


**Fig. 5** (a, b) SEM micrographs of the sample 1 after 3 h of heating in microwave oven and a thermal treatment at  $300\text{ }^\circ\text{C}$

grade of HAp is good enough, and at the same time a high enough proportion of HAp is maintained. The mineralogical composition of the thermally treated samples can be seen in Fig. 7.

In the case of sample 1, it two crystalline phase results by thermal treatment:  $\text{Ca}_3\text{P}_2\text{O}_8$  with intense lines and HAp in a much smaller proportion. Relating to the sample with MgO as additive, a solid solution of  $\text{Ca}_3\text{P}_2\text{O}_8$  with MgO was formed, which confirms the data obtained in the paper [22]. At the same time, it may be noticed that in the sample with MgO, HAp exists in a greater quantity being stabilised by partial substitution of  $\text{Mg}^{2+}$  ion in its lattice, in accordance with the data from paper [18].

The two samples were analysed by FTIR spectroscopy and the curves were showed in Fig. 8.

One can notice bands specific for the  $[\text{PO}_4^{3-}]$  group and respectively  $[\text{HO}^-]$  from HAp structure in case of the sample without MgO. At the same time, bands specific at  $1,087$  and  $1,032\text{ cm}^{-1}$  which are specific for  $\beta\text{-Ca}_3\text{P}_2\text{O}_8$  appeared. Bands characteristic for  $\text{HO}^-$  ion in HAp lattice and for adsorbed water can be also seen. The presence of a large band centred at  $3,460\text{ cm}^{-1}$ , with a much weaker intensity shows, after the thermal treatment at  $1,200\text{ }^\circ\text{C}$ , a smaller quantity of HAp, fact which confirms the results obtained by X-ray diffraction. For the sample with MgO,

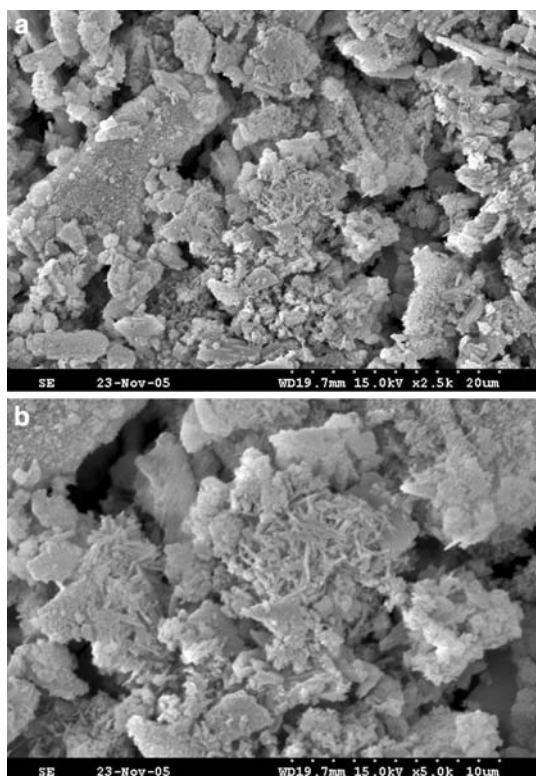


**Fig. 6** (a, b) SEM micrographs of the sample 2 after 3 h of heating in microwave oven and thermally treated at 300 °C

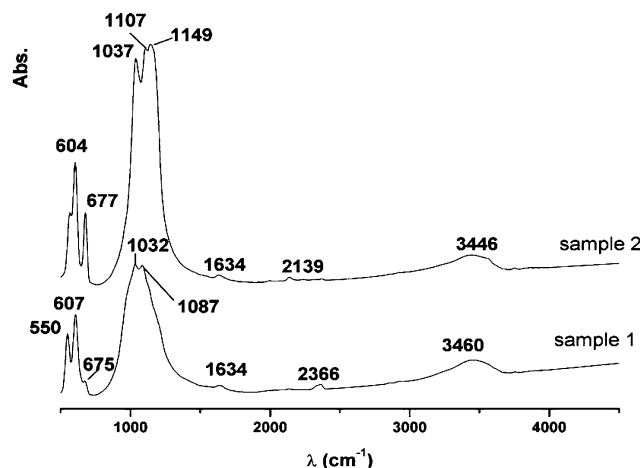


**Fig. 8** FTIR spectra of samples 1 and 2 thermally treated at 1,200 °C

Needle-like or prismatic grains (Fig. 9b) show HAP presence respectively nucleation and growth of  $\beta$ - $\text{Ca}_3\text{P}_2\text{O}_8$  on their surface. The presence of pores at the limit between grains was noticed.

In the sample with MgO, as sintering additive, the presence of two types of grains was seen; some of these are similar with those from the stoichiometric sample

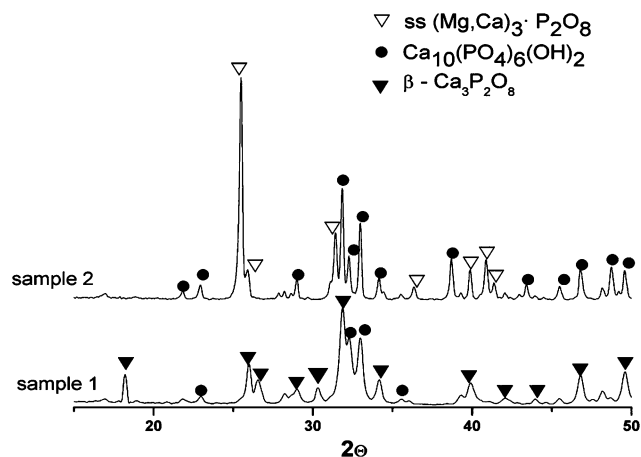


**Fig. 7** XRD patterns for the samples 1 and 2, thermally treated at 1,200 °C

one can notice that the line specific for  $\text{HO}^-$  from HAp ( $677\text{ cm}^{-1}$ ) is more intense compared to the previous sample, in accordance with the results obtained by X-ray diffraction. This fact shows that in this sample HAp exists in a proportion much greater than in sample 1.

The texture of the samples thermally treated at 1,200 °C was examined by the electronic microscope SEM. For sample 1 (Fig. 9a), regular grains with variable dimensions (2–6  $\mu\text{m}$ ), corresponding to  $\beta$ - $3\text{CaO}\cdot\text{P}_2\text{O}_5$ , can be seen.

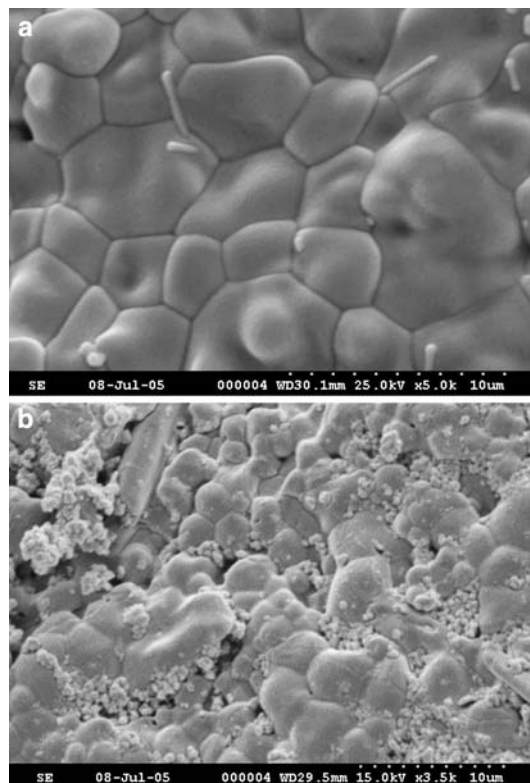


**Fig. 9** SEM micrographs of the sample 1 thermally treated at 1,200 °C; (a) sectional view; (b) sample surfaces

**Fig. 10** SEM micrographs for sample 2 thermally treated at 1,200 °C. (a) sample surfaces; (b) sample surfaces; (c) sectional view

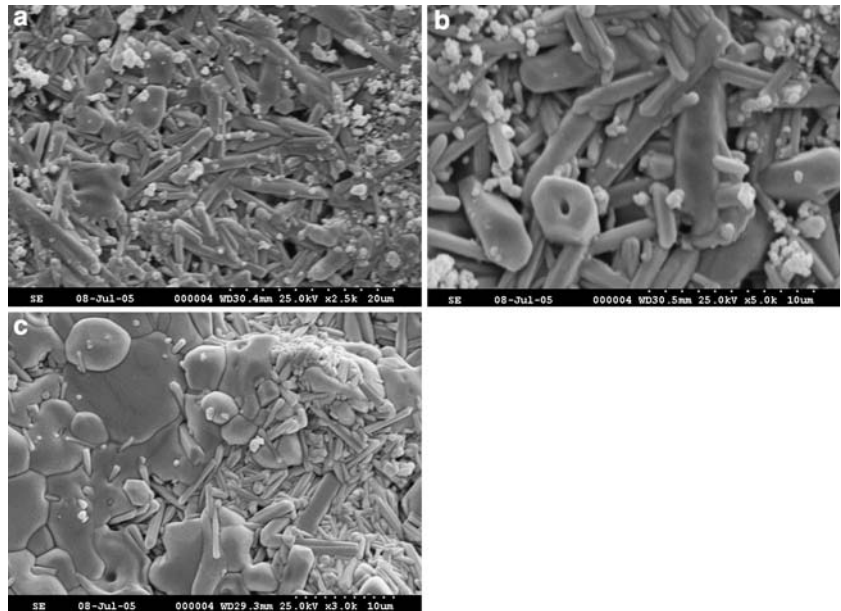


(Fig. 10). In Fig. 10a, b can see prismatic HAp grains. On their surface it is observed the nucleation and development of tricalcium phosphate.

Other long grains (Fig. 10c), show the morphology of the initial powder, and this fact confirms the results from papers [22, 23]. This finding is confirmed by X-ray diffraction studies, which show the presence of two phases,  $\beta$ - $\text{Ca}_3\text{P}_2\text{O}_8$  and HAp in this sample. In this case, the presence of inters and intra-grain pores can be observed.

## Conclusions

From the undertaken studies it was concluded that HAp could be obtained after 3 h of microwave heating starting from  $\text{CaSO}_4 \cdot 2\text{H}_2\text{O}$ ,  $\text{Ca}(\text{OH})_2$  and  $(\text{NH}_4)_2\text{HPO}_4$ . There are two stages of the reactions which lead to its forming. After 1 h the presence of  $\text{CaHPO}_4$ , an intermediate phase was noticed, which then reacted with  $\text{Ca}(\text{OH})_2$  found in excess and lead to the HAp formation. X-ray diffraction and FTIR specific bands evidenced hydroxyapatite. The scanning electron microscopy showed that for the processed powders a special morphology was obtained that is needle-like shape. After a thermal treatment at 1,200 °C with 1-h plateau, HAp passes in a high proportion in  $\beta$ - $\text{Ca}_3\text{P}_2\text{O}_8$ , result obtained by X-ray diffraction and confirmed also by the electron microscopic investigations. By use of 1.05 wt% MgO in composition of samples hydroxyapatite is stabilised. At 1,200 °C this can be found in a greater proportion as needle-like grains in comparison with stoichiometric sample.

## References

1. I. TEOREANU, E. ANDRONESCU and A. FOLEA, *Ceram. Intern.* **22** (1996) 305
2. P. PARHI, A. RAMANAN and A. R. RAY, *Mater. Lett.* **58** (2004) 3610
3. S. KOMARNENI and H. KATSUKI, *Pure Appl. Chem.* **74** (2002) 1537
4. D. S. R. KRISHNA, C. K. CHAITANYA, S. K. SESHADRI and T. S. S. KUMAR, *Trends Biomater. Artif. Organs.* **16** (2002) 15
5. S. Y. YOON, Y. M. PARK, S. S. PARK, R. STEVENS and H. C. PARK, *Mater. Chem. Phys.* **91** (2005) 48
6. H. KATSUKI and S. FURUTA, *J. Amer. Ceram. Soc.* **82** (1999) 2257
7. M. PREDA, A. MELINESCU, I. TEOREANU and M. ZAHARESCU, *Rom. J. Mater.* **34** (2004) 3
8. L. C. CHOW, L. SUN and B. HOCKEY, *J. Res. Natl. Inst. Stand. Technol.* **109** (2004) 543
9. M. MARCOVIC, B. O. FOWLER and M. S. TUNG, *J. Res. Natl. Inst. Stand. Technol.* **109** (2004) 553
10. A. LOPEZ-MACIPE, R. RODRIGUEZ-CLEMENTE, A. HIDALGO-LOPEZ, I. ARITA, M. V. GARCIA GARDUNO, E. RIVERA and V. M. CASTANO, *J. Mater. Synth. Process* **6** (1998) 21
11. I. REHMAN and W. BONFIELD, *J. Mater. Sci. Mater. Med.* **8** (1997) 1
12. A. SIDDHARTAN, K. S. SESHADRI and T. S. SAMPATH KUMAR, *J. Mater. Sci. Mater. Med.* **15** (2004) 1279
13. M. WEI, J. H. EVANS, T. BOSTROM and L. GRONDHL, *J. Mater. Sci. Mater. Med.* **14** (2003) 311
14. S. RAYNAUD, E. CHAMPION, D. BERNACHE-ASSOLLANT and P. THOMAS, *Biomaterials* **23** (2002) 1065
15. M. TAMAI, M. NAKAMURA, T. ISSIKI, K. NISHIO, H. ENDOH and A. NAKAHIRA, *J. Mater. Sci. Mater. Med.* **14** (2003) 617
16. A. SLOSARCZYK and J. BIALOSKORSKI, *J. Mater. Sci. Mater. Med.* **9** (1998) 103
17. I. R. GIBSON, S. KE, S. M. BEST and W. BONFIELD, *J. Mater. Sci. Mater. Med.* **12** (2001) 163

18. M. A. FANOVICI and J. M. PORTO LOPEZ, *J. Mater. Sci. Mater. Med.* **9** (1998) 53
19. P. N. KUMTA, Ch. SFEIR, D. H. LEE, D. OLTON and D. CHOI, *Acta Biomaterialia* **1** (2005) 65
20. I. TEOREANU, M. PREDA and A. MELINESCU, *Rev. Chim.* **56** (2005) 1205
21. I. TEOREANU, M. PREDA and A. MELINESCU, *Key Eng. Mater.* **264–268** (2004) 2091
22. R. Z. LEGEROS, S. LIN, R. ROHANIZADEH, D. MIJARES and J. P. LEGEROS, *J. Mater. Sci. Mater. Med.* **14** (2003) 201
23. T. A. KURIAKOSE, S. N. KALCURA, M. PALANICHAMY, D. ARIVUOLI, K. DIERKS, G. BOCELLI and C. BETZEL, *J. Cryst. Growth*, **263** (2004) 517